

# Experimental report

08/04/2020

**Proposal:** DIR-181

**Council:** 4/2019

**Title:** Defect-induced activity of  $(\text{La}_{0.6-x}\text{Ce}_x\text{Sr}_{0.4})(\text{Ce}_y\text{Mn}_{1-y})\text{O}_3$ , a promising perovskite redox material class for solar thermochemical  $\text{CO}_2$  splitting

**Research area:** Chemistry

**This proposal is a new proposal**

**Main proposer:** Madhusudhan Naik JARPLA

**Experimental team:** Madhusudhan Naik JARPLA  
Devi Prasad ADIYERI SASEENDRAN

**Local contacts:** Clemens RITTER

**Samples:** pure  $\text{La}_{0.6}\text{Sr}_{0.4}\text{MnO}_3$   
40% Ce-substituted  $\text{La}_{0.6}\text{Sr}_{0.4}\text{MnO}_3$   
25% Ce-substituted  $\text{La}_{0.6}\text{Sr}_{0.4}\text{MnO}_3$

Instrument	Requested days	Allocated days	From	To
D2B	5	3	07/10/2019	10/10/2019

## Abstract:

Solar thermochemical  $\text{CO}_2/\text{H}_2\text{O}$  splitting has the potential to generate industrial scale synthetic liquid fuels and reduce global warming emissions. However, material innovations that can overcome thermodynamic limitations of current class of redox materials are required to increase efficiencies. Perovskites oxide materials are currently emerging as alternate class of redox materials to ceria, mainly because of its thermodynamic and structural tuning derived through engineered composition. Here we have identified a novel class of Ce-substituted perovskite redox materials  $\text{La}_{0.6}\text{Sr}_{0.4}\text{MnO}_3(\text{LSM})$ , which can overcome the individual limitations of ceria and perovskites. Amongst them, 25% Ce-substituted  $\text{La}_{0.6}\text{Sr}_{0.4}\text{MnO}_3$  displayed 3 times higher reduction extent than pure ceria and 2 times faster re-oxidation kinetics than pure LSM perovskite during TGA redox cycling experiments at lower reduction temperatures (1673 K). The experiment involves the use of D2B neutron diffractometer under high temperature reaction conditions (1623 K) aimed to elucidate the defect-induced activity correlation, along with determining exact occupancies of Ce at A-site at B-site & monitoring structural distortions.

## Defect-induced activity of $\text{La}_{0.60-x}\text{Sr}_{0.40+x}\text{Ce}_y\text{Mn}_{1-y}\text{O}_3$ ( $y= 0, 0.10, 0.25$ ), a promising perovskite oxide redox material class for solar thermochemical $\text{CO}_2$ splitting

*J. Madhusudhan Naik<sup>1</sup>, Greta R. Patzke<sup>1</sup>*

<sup>1</sup>*Department of Chemistry, University of Zurich, Winterthurerstrasse 190, CH-8057 Zurich, Switzerland*

We have carried out in-situ high temperature neutron diffraction experiments with the goal of elucidating the structure of novel ceria-substituted perovskite oxides. Three samples namely, pure LSM, 10 % Ce and 25 % Ce- substituted  $\text{La}_{0.60-x}\text{Sr}_{0.40+x}\text{Ce}_y\text{Mn}_{1-y}\text{O}_3$ , were tested on high resolution D2B neutron diffractometer using 1.6 Å & 1.05 Å wavelength beam. In-situ high temperature measurements were recorded at two different temperatures 1350 °C and 1000 °C using standard niobium furnace (under vacuum conditions of  $10^{-4}$ - $10^{-5}$  mbar). These experimental conditions simulate the working conditions of a concentrated solar power reactor as well as experimental testing conditions using thermogravimetric (TGA) analyser. These in-situ high temperature neutron diffraction measurements data have helped in monitoring temperature induced phase transitions and understanding structure of sample at real working conditions. We have identified and confirmed the substitution of  $\text{Ce}^{4+}$  ions at the B-site (12 % Ce in LSC25M75) of the perovskite composition (thereby distinguishing  $\text{La}^{3+}$  and  $\text{Ce}^{4+}$  ions), determined exact atomic occupancy of Ce, Mn and Oxygen ions (oxygen vacancy defects) along with monitoring octahedral structural distortions.

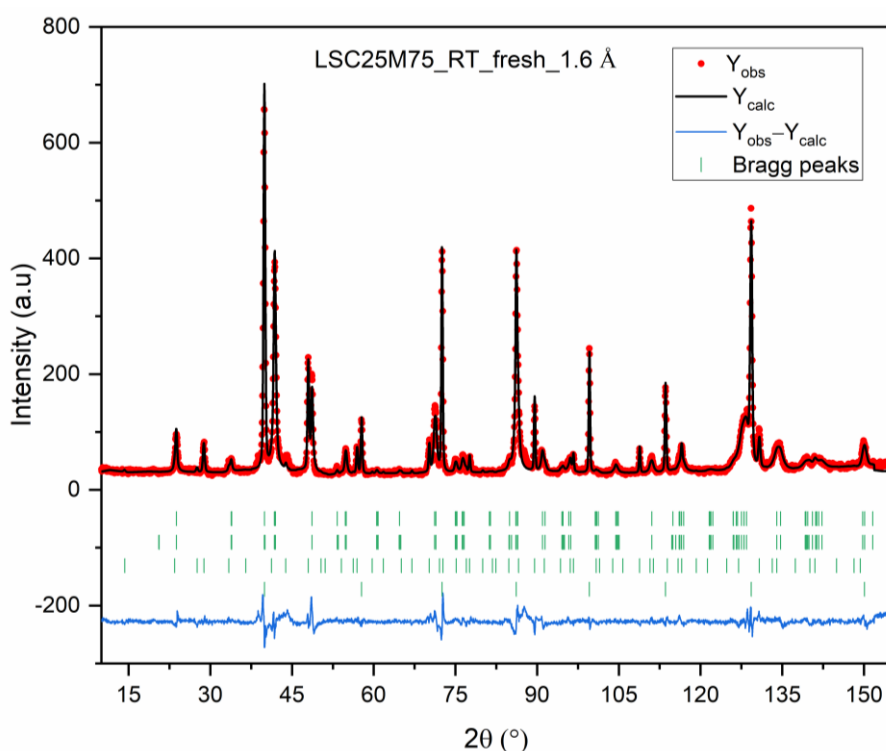


**Fig 1.**  $\text{La}_{0.48}\text{Sr}_{0.52}(\text{Ce}_{0.12}\text{Mn}_{0.88})\text{O}_{2.55}$  ( $R\text{-}3c$ , 72.5%);  $a = 5.4775(3)$  Å,  $c = 13.3548(12)$  Å, volume =  $347.925(3)$  Å<sup>3</sup>,  $\text{Ce}_{1.6}\text{La}_{0.4}\text{O}_{7.8}$  ( $Fd\text{-}3m$ , 27.5%);  $a = 11.0875(3)$ ;  $R_{wp} = 9.28$  %,  $R_p = 6.93$  %,  $\chi^2 = 4.32$

## DIR-181 Experimental report

Atom	Site	<i>x</i>	<i>y</i>	<i>z</i>	Occ.	Atomic displacement (anisotropic) parameters (Å <sup>2</sup> )					
						<i>U</i> <sup>11</sup>	<i>U</i> <sup>22</sup>	<i>U</i> <sup>33</sup>	<i>U</i> <sup>12</sup>	<i>U</i> <sup>13</sup>	<i>U</i> <sup>23</sup>
La	6a	0.00000	0.00000	0.25000	0.48	0.005(3)	0.005(3)	0.004(3)	0.002(3)	0.000	0.000
Sr	6a	0.00000	0.00000	0.25000	0.52	0.005(3)	0.005(3)	0.004(3)	0.002(3)	0.000	0.000
Mn	6b	0.00000	0.00000	0.00000	0.88(2)	0.041(8)	0.041(8)	-0.060(2)	0.020(8)	0.000	0.000
Ce	6b	0.00000	0.00000	0.00000	0.12(2)	0.041(8)	0.041(8)	-0.060(2)	0.020(8)	0.000	0.000
O	18e	0.4727(2)	0.00000	0.25000	0.85(3)	0.005(2)	0.016(4)	0.001(2)	0.008(4)	-0.003(1)	-0.006(1)

**Table 1.** La<sub>0.48</sub>Sr<sub>0.52</sub>(Ce<sub>0.12</sub>Mn<sub>0.88</sub>)O<sub>2.55</sub>, Space group: *R*-3*c*, *a* = 5.4775(3) Å, *c* = 13.3548(13) Å, volume = 347.925(3) Å<sup>3</sup>, *R*<sub>wp</sub> = 9.28 %, *R*<sub>p</sub> = 6.93 %,  $\chi^2$  = 4.32

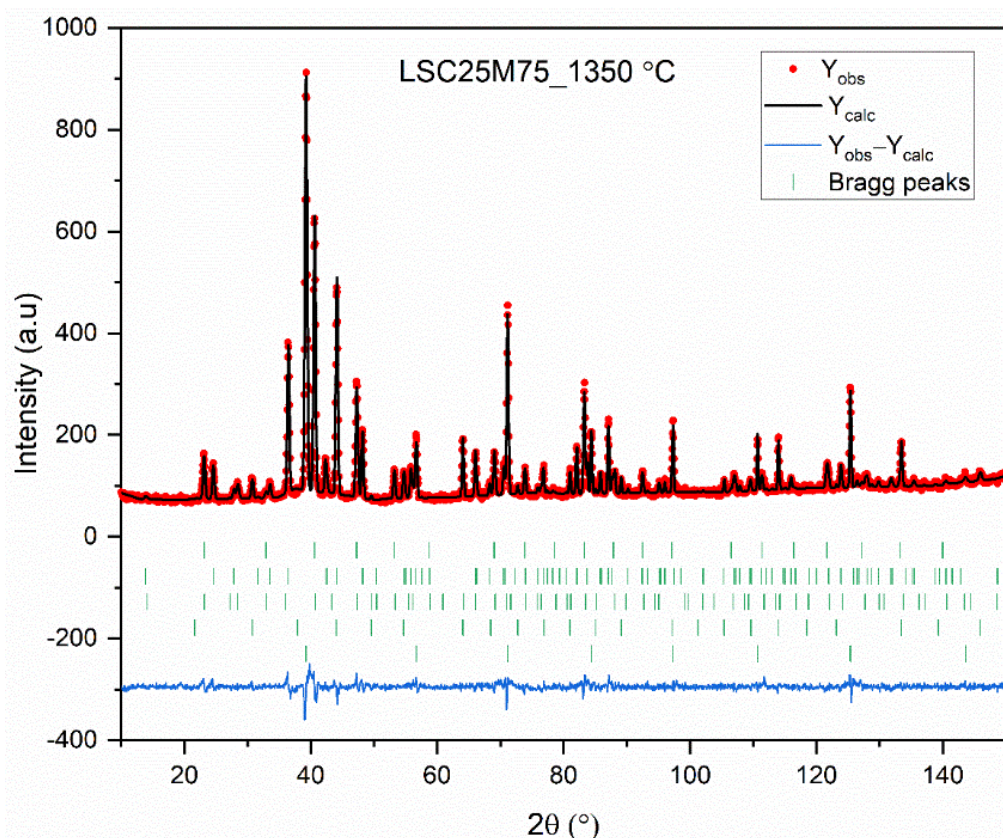


**Fig 2.** La<sub>0.48</sub>Sr<sub>0.52</sub>MnO<sub>3</sub> (*P*-*m*3*m*, 41%), *a* = 3.9783(1) Å, volume = 62.965(3) Å<sup>3</sup>; (Sr<sub>1.10</sub>La<sub>0.65</sub>Ce<sub>0.25</sub>)MnO<sub>3.90</sub> (*I*4/*mmm*, 47 %), *a* = 3.9042(1) Å, *c* = 13.2443(6) Å, volume = 201.885(1) Å<sup>3</sup>; Ce<sub>1.6</sub>La<sub>0.4</sub>O<sub>7-8</sub> (*Fd*-3*m*, 12 %) *a* = 11.2295(6); volume = 1416.059(14) Å<sup>3</sup>; *R*<sub>wp</sub> = 4.85 %, *R*<sub>p</sub> = 3.60 %,  $\chi^2$  = 2.44

At 1350 °C and 1000 °C, the *R*-3*c* phase transformed into *Pm*-3*m* and *I*4/*mmm*, along with *Fd*-3*m* phase (8-12 %) present as an oxide ion conductor. Especially, the structure at 1000 °C has a predominant (Sr<sub>1.18</sub>La<sub>0.60</sub>Ce<sub>0.22</sub>)MnO<sub>3.97</sub>, *I*4/*mmm* (~ 70 %) phase and provides important information about the material structure at similar conditions as in a solar reactor after cooling down from the reduction temperature 1350 °C.

## DIR-181 Experimental report

All the high temperature measurements were carried out only using 1.6 Å wavelength beam, as the lower wavelength 1.05 Å pattern resulted in poor resolution of peaks at high  $2\theta$  values (large  $q$ -space).

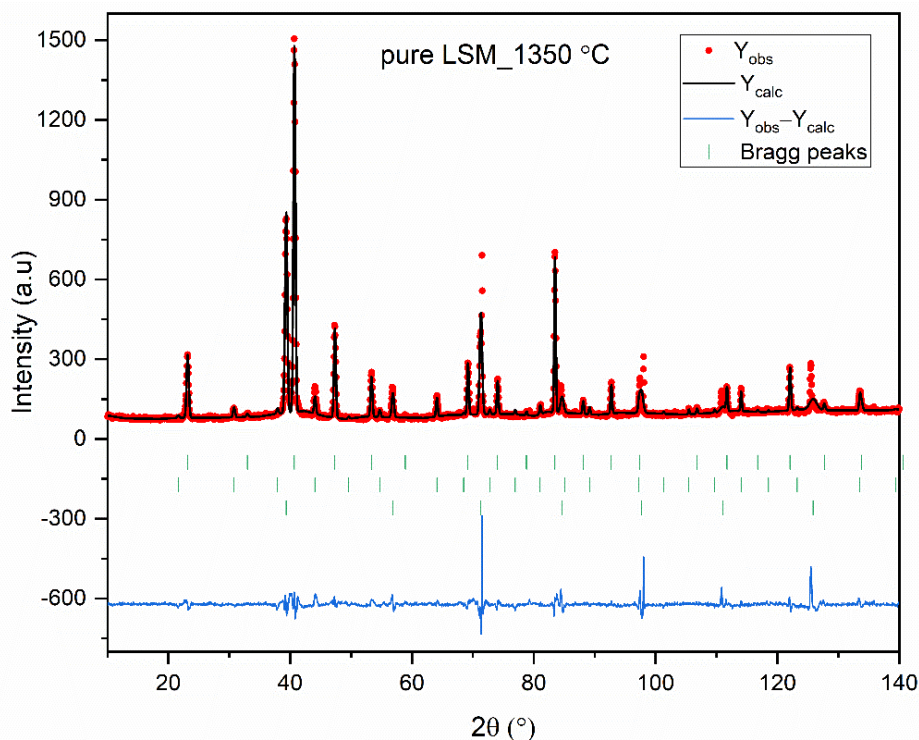


**Fig 3.** Pure LSM sample at 1350 °C,  $\text{La}_{0.60}\text{Sr}_{0.40}\text{MnO}_3$  ( $Pm\bar{3}m$ , 95 %),  $a = 3.9705(1)$  Å, volume = 62.596(3) Å<sup>3</sup>;  $\text{NbO}$  or  $\text{SrNbO}_{3-\delta}$  ( $Pm\bar{3}m$ , 5 %)  $a = 4.2488(2)$  Å, volume = 76.698(6);  $R_{wp} = 8.83$  %,  $R_p = 5.57$  %,  $\chi^2 = 8.60$

The pure LSM sample ( $\text{La}_{0.60}\text{Sr}_{0.40}\text{MnO}_3$ ) diffraction experiment at 1350 °C resulted in complete transformation of single phase room temperature rhombohedral phase ( $R\bar{3}c$ ) to cubic ( $Pm\bar{3}m$ ), however there is an additional impurity phase (~ 5 %), possibly due to partial oxidation of niobium sample container at high temperatures. The presence of this impurity phase is surprising for us, as the niobium sample container is maintained at  $10^{-4}$ - $10^{-5}$  mbar vacuum conditions during high temperature measurements. We have also observed brownish coating on the inner walls of the sample container after the high temperature measurement of the pure LSM sample. The amount of lattice oxygen evolved from the manganite perovskite oxide sample is considered generally very low. In addition, we did not observe any impurity phase after thermogravimetric (TGA) analysis of the same samples tested in our lab. These arguments lead us to assume that the only possibility of formation of oxide impurity phase could be due to the lattice oxygen released from the sample and that the vacuum could have been slightly fluctuated during the measurements.

Finally, two manuscripts derived from these in-situ measurements are in preparation.